Available online at www.sciencedirect.com
ScienceDirect
Biomaterials 28 (2007) 1–8
Biomaterials
www.elsevier.com/locate/biomaterials

Preparation and characterization of cross-linked collagen–phospholipid polymer hybrid gels

Kwangwoo Nam, Tsuyoshi Kimura, Akio Kishida*

Division of Biofunctional Molecules, Institute of Biomaterials and Bioengineering, Tokyo Medical and Dental University, 2-3-10 Kanda-Surugadai, Chiyoda-ku, Tokyo 101-0062, Japan

Received 5 June 2006; accepted 1 August 2006
Available online 7 September 2006

Abstract

2-methacryloyloxyethyl phosphorylcholine (MPC)-immobilized collagen gel was developed. Using 1-ethyl-3-(3-dimethyl aminopropyl)-1-carbodiimide hydrochloride (EDC) and *N*-hydroxysuccinimide (NHS), we cross-linked a collagen film in 2-morpholinoethane sulfonic acid (MES) buffer (EN gel). EN gel was prepared under both pH 4.5 and pH 9.0 in order to observe changes in cross-linking ability. To cross-link MPC to collagen gel, poly(MPC-*co*-methacrylic acid) (PMA) having a carboxyl group side chain was chosen. E/N gel was added to the MES buffer having pre-NHS activated PMA to make MPC-immobilized collagen gel (MiC gel). MiC gel was prepared under both acidic and alkaline conditions to observe the changes in the cross-linking ability of PMA. X-ray photoelectron spectroscopy showed that the PMA was cross-linked with collagen under both acidic and alkaline conditions. Differential scanning calorimetry (DSC) results showed that the shrinkage temperature increased for the MiC gels and that the increase would be greater for the MiC gel prepared under alkaline conditions. The data showed that swelling would be less when the MiC gel was prepared under alkaline conditions. The biodegradation caused by collagenase was suppressed for the MiC gel prepared under alkaline conditions due to stable inter- and intrahelical networks.
© 2006 Elsevier Ltd. All rights reserved.

Keywords: Collagen; Phospholipid; Cross-linking; Surface modification

1. Introduction

Collagen is an extracellular-matrix protein that plays an important role in the formation of tissues and organs and is involved in various functional expressions of cells [1]. Collagen is non-toxic, non-antigenic, favors cell adhesion, proliferation, and differentiation to mimic the natural cell environment. However, favoring cell adhesion can be both advantageous and disadvantageous, for its strong affinity to cells and blood is uncontrollable, which may soon lead to blood coagulation and mineralization when applied for use as artificial blood vessels. Furthermore, the collagen that is prepared in a matrix form such as a gel for tissue reconstruction is mechanically insufficient [2]. Without modification, the collagen gel cannot be applied for bioprosthesis [3].

To overcome the disadvantages of collagen while maintaining its biological performance, a prosthesis-tissue complex, or bioartificial polymeric material, was developed by blending or mixing biomolecules and synthetic materials. The chief purpose for developing such a bioartificial polymer material is to overcome the poor biological performance of synthetic polymers and to enhance the mechanical characteristics of biomolecules [4].

To control cell adhesiveness and to increase mechanical strength simultaneously, collagen must be modified by cross-linking or mixing with synthetic polymers. Polymers such as poly(vinyl alcohol), poly(acrylic acid), poly(vinyl pyrrolidone), and polyethylene are used as bioartificial polymer materials because of their favorable chemical reactivity with collagen, absence of toxicity, and good mechanical performance [4–8].

However, it is very important to consider biological response in the adoption of a cross-linker or synthetic polymer because of the possibilities of severe problems

*Corresponding author. Tel./fax: +81 03 5280 8028.
E-mail address: kishida.fm@tmd.ac.jp (A. Kishida).

0142-9612/$ - see front matter © 2006 Elsevier Ltd. All rights reserved.
doi:10.1016/j.biomaterials.2006.08.002

such as toxicity, inflammatory response, or alteration of protein structure. Furthermore, some synthetic polymers that are known to be 'biocompatible' degrade in biological fluids, making the collagen structure unstable. Adoption of natural cross-linkers such as glutaraldehyde [9], genipin [10], or transglutaminase [11], and natural polymers like hyaluronic acid [12], heparin [13], or chondroitin-6-sulfate [14,15] is used as direct cross-linker or immobilizer to overcome the problems presented by the use of synthetic polymers, but cannot fully solve the problems.

To overcome these problems, we developed a biosynthetic hybrid material by cross-linking collagen with a 2-methacryloyloxyethyl phosphorylcholine (MPC) based copolymer using *N*-(3-dimethylaminopropyl)-*N'*-ethylcarbodiimide (EDC) and *N*-hydroxysuccinimide (NHS) as cross-linkers by activating the MPC polymer with EDC and NHS to cross-link the microfibrils and polymer chain using amide bond [3,16–18].

MPC is a blood compatible product developed in the early 1990s [19]. Design of the MPC polymer took into account the surface structure of the biomembrane. Recently, phospholipid-accumulated surfaces have been prepared by various methods, and it has been reported that the phosphorylcholine group plays an important role showing excellent blood compatibility and anti-protein adsorptivity [20–23]. The MPC units can then be introduced to conventional polymers by various methods of modification. They effectively reduce protein adsorption and denaturation and inhibit cell adhesion even when the polymer is exposed to whole blood in the absence of any anticoagulants [24]. By adopting the MPC polymer with the collagen gel, it is possible to expect a biocompatible collagen–polymer hybrid gel that is stable, has its molecular weight controlled, has no cross-linker leaking, and is mechanically tough.

In the present study, cross-linking ability between poly(MPC-*co*-methacrylic acid) (PMA) and collagen using EDC and NHS was investigated by altering several parameters, and the physical properties of PMA-immobilized matrices were characterized. In this article, the terms interchain cross-linking and immobilization are used synonymously.

2. Experimental method

2.1. Preparation of collagen–phospholipid polymer hybrid gel

2.1.1. Synthesis of PMA

PMA was synthesized by a method that has already been published [19]. In short, desired amount of MPC and MA was dissolved in ethanol in an ampoule. Then 2,2'-azoisobutyronitrile (AIBN) was added to the ethanol solution. The argon gas was bubbled into the ethanol solution to eliminate the oxygen. The ampoule was sealed and heated to 60 °C for 16 h. The solution was precipitated into diethyl ether, freeze-dried, and kept in vacuum until use. The mole ratio of PMA was controlled to MPC:MA = 3:7, and the number average molecular weight $\overline{M}_n$ of the PMA was approximately 300,000. The chemical structure of PMA is shown in Fig. 1.

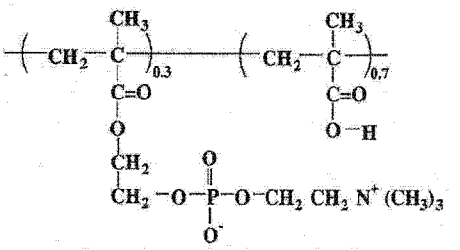

Fig. 1. Chemical structure of PMA.

Table 1
Terminology of collagen gels used in this study

Terminology	Composition
Uc-gel	Uncross-linked collagen gel (immersed in alkaline pH conditions)
EN-1	EDC/NHS-cross-linked collagen gel under acidic pH conditions
EN-2	EDC/NHS-cross-linked collagen gel under alkaline pH conditions
MiC-11 gel	PMA immobilized to EN-1 gel under acid pH conditions
MiC-12 gel	PMA immobilized to EN-1 gel under alkaline pH conditions
MiC-21 gel	PMA immobilized to EN-2 gel under acid pH conditions
MiC-22 gel	PMA immobilized to EN-2 gel under alkaline pH conditions

2.1.2. Preparation of EDC and NHS cross-linked collagen gel (EN gel)

Cross-linked collagen gel was prepared by using 0.5 wt% collagen type I solution (pH 3, KOKEN, Tokyo, Japan). Conventional film fabrication method was used for the film fabrication. The collagen solution was dropped onto the polyethylene film and dried in room temperature. The collagen film (thickness = 36±2 μm) was immersed into a 0.05 M 2-morpholinoethane sulfonic acid (MES) buffer (pH 4.5) (Sigma, St. Louis, USA) containing 1-ethyl-3-(3-dimethyl aminopropyl)-1-carbodiimide hydrochloride (EDC) (Kanto Chemicals, Tokyo, Japan) and NHS (Kanto Chemicals, Tokyo, Japan). Each chemical was added at the mole ratio of EDC:NHS:collagen-carboxylic acid groups = 5:5:1 [11,13]. The cross-linking procedure was allowed to continue for 4 h at 4 °C to produce a cross-linked gel (EN-1 gel). After 4 h, the reaction was stopped by removing the gel from the solution. The gel was then washed with 4 M of Na_2HPO_4 aqueous solution for 2 h to hydrolyze any remaining *O*-acylisourea groups and then with distilled water for 3 days to remove any salts from the gel. Same preparation process was repeated under alkaline conditions (pH 9.0; adjusted with NaOH) to prepare an EN-2 gel.

2.1.3. Preparation of MPC-immobilized collagen gel (MiC gel)

Preparation of the MiC gel was done by using the EN-1 and EN-2 gels. PMA was added with EDC and NHS to the MES buffer (pH 4.5 and pH 9.0) and was pre-activated for 10 min before immersion of the EN-1 or EN-2 gel. The immobilization of PMA to the collagen was allowed to continue for 4 h at 4 °C. The gel was then washed with 4 M of Na_2HPO_4 aqueous solution for 2 h and then with distilled water for 1 day to remove any salts from the gel to prepare a salt-free MiC gel: MiC-11 gel (PMA immobilized under acidic conditions using the EN-1 gel), MiC-12 gel (PMA immobilized under alkaline conditions using the EN-1 gel), MiC-21 gel (PMA immobilized under acidic conditions using the EN-2 gel), and MiC-22 gel (PMA immobilized under alkaline conditions using the EN-2 gel). The terminology of the samples is listed in Table 1. PMA cross-linking with the collagen is shown in Fig. 2. Collagen film was immersed

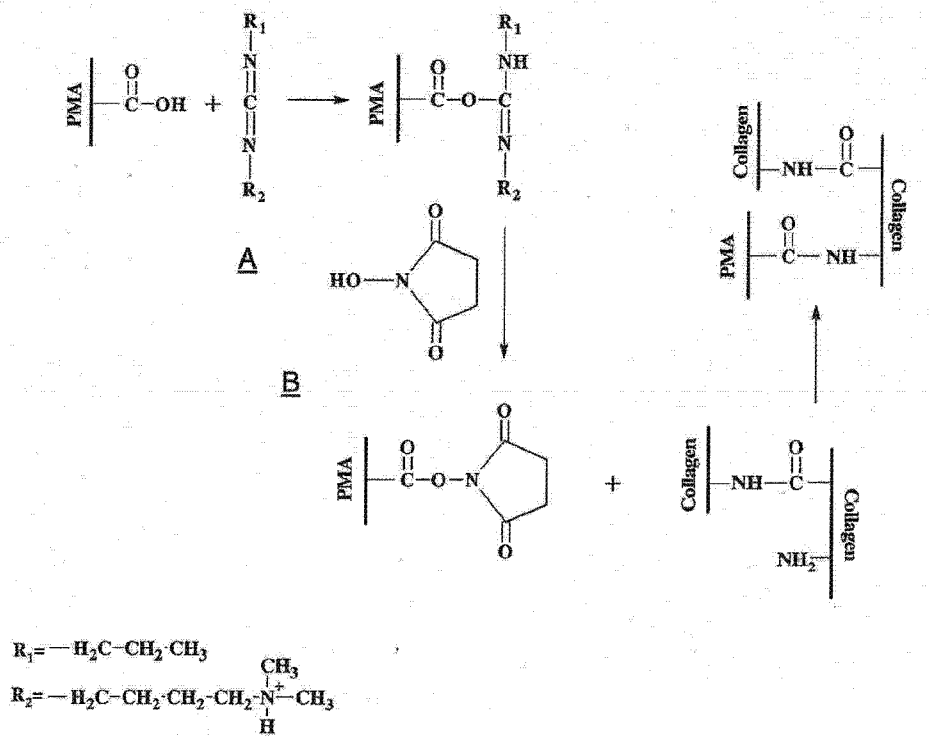

A: 1-ethyl-3-(3-dimethylaminopropyl)-1-ethylcarbodiimide hydrochloride (EDC)
B: *N*-hydroxysuccinimide (NHS)

Fig. 2. Schematic picture of immobilization of MPC polymer with collagen.

into the MES buffer pH 9.0 for 1 day to obtain a non cross-linked collagen gel (Uc-gel) and was used as a reference.

2.2. Characterization

2.2.1. Surface analysis

Surface analysis was executed using X-ray photoelectron spectroscopy (XPS, AXIS-HSi, Shimadzu/KRATOS, Kyoto, Japan) and scanning electron microscopy (SEM, SM-200, Topcon, Tokyo, Japan). The samples, which had been cut into small pieces, were lyophilized overnight. The chemical composition of the surfaces of the gel was determined by the take-off angle of the photoelectrons fixed at 90°. The morphologies of the gels were observed with SEM after gold coating with an ion coater (IB-3, Eiko Co., Ibaraki, Japan). The razor blade-cut surfaces of the respective gels were observed.

2.2.2. Shrinkage temperature

The shrinkage temperatures of the gels were determined using differential scanning calorimetry (DSC, DSC6000, Seiko, Chiba, Japan) in the range 0–150 °C at a scanning rate 5 °C/min. The samples were incubated with small amounts of phosphate buffer solution for 1 h at room temperature before being measured [9]. Instead of an empty container, a container of PBS was used for reference.

2.2.3. Mechanical properties

The stress–strain curves of the respective collagen gels were determined by uniaxial measurements using a universal testing machine (Orientec STA-1150, Tokyo, Japan). The sizes of the samples used for measurement were 4 cm × 1 cm. Each sample was strained at the rate of 10 mm/min. The obtained data were fitted to the stress–strain curves of the samples and the elongational modulus at 1% and 8% was calculated.

2.2.4. Swelling test

A swelling test of each sample was executed by cutting the lyophilized gels into small pieces and putting them into pH-controlled aqueous solutions at 37 °C. The pH of the aqueous solution was controlled to 2.1 or 7.4. The gels were gently shaken for 24 h and then removed for weighing. The swelling ratio was calculated in order to define the exact amount of swelling caused by water absorption. The equation used for the swelling ratio was

$$\text{Swelling ratio, } S(\%) = \frac{W_h - W_d}{W_d} \times 100$$

where W_h is hydrated weight and W_d is dried weight of the gel.

2.2.5. Enzymatic degradation test

Degradation tests of the gel samples were executed using collagenase from Clostridiopeptidase histoluticum (EC 3.4.24.3, *Sigma*, St. Louis, USA) with collagenase activity of 300 units/mg. In this experiment, 30±2 mg of collagen gels were immersed into 2 mL of 0.1 M Tris-HCl buffer (pH 7.4) with 5×10^{-3} M of calcium chloride (Kanto Chemical, Tokyo, Japan) and 8×10^{-4} M of sodium azide (Kanto Chemicals, Tokyo, Japan) and was shaken for 1 h at 37 °C. Then, 2 mL of collagenase Tris-HCl buffer solution with a concentration of 1.32 mg/mL was added to the solution containing the gel to determine the total concentration of collagenase at 100 units/mL. The container was returned to the shaking water bath. The remaining weights of the samples were measured for 72 h.

2.2.6. Statistical analysis

All experiments were repeated at least three times and the values are expressed as mean ±standard deviation. In several figures, the error bars are not visible because they are included in the plot. Statistical analyses were performed using student's *t*-test. The level of significance was set as $P<0.05$.

3. Results and discussion

3.1. Basic characteristics of collagen gels

The reaction between EDC and the carboxyl groups are shown elsewhere; the mechanism is well known [25,26]. According to Nakajima and Ikada [26], proton and ionized carboxyl groups are required for the reaction with EDC. The excess amount of EDC against the carboxyl groups should be used up, and no reaction occurred when the molar ratio of EDC to the carboxyl groups was below 0.5. Using EDC for cross-linking might cause hydrolysis, which makes the carboxyl groups return to the original carboxyl groups.

The use of NHS is to prohibit the hydrolysis of the carboxyl groups. NHS would lead to formation of NHS-ester, which prevents the side reaction of the *O*-acylisourea groups [25,26]. This is because the reactive species relative to the neucleophilic attack of the free amine group of collagen are the NHS-activated carboxyl groups rather than the *O*-acylisourea groups.

Fig. 3 shows the XPS result of Uc-gel, EN-2 gel, MiC-21 gel, and MiC-12. All gels showed XPS signals attributed to carbon in CH_3– or –CH_2–, –COC–, C(=O)–, and nitrogen in –CONH– was observed at 285, 286.6, 288.5, and 400.8 eV, respectively. The phosphorus peak and one nitrogen peak in $-N^+(CH_3)_3$ were observed at 134 and 403.2 eV, respectively, indicating that PMA was a properly cross-linked collagen [21,24].

SEM images of the outer surfaces and razor blade-cut surfaces (vertical cross-section) of the respective collagen gels are shown in Fig. 4. The razor blade-cut surfaces of the Uc-gel and the EN-1 and EN-2 gels are porous. For MiC, the non-porous layer is shown to be deposited on the porous layer. Non-porosity can be seen for the pure PMA film prepared using same method (image not shown). This implies that PMA covers the collagen gel instead of being blended, making it a heterogeneous phase. However, the outer surface of the gel is entirely one phase showing no defects, indicating that PMA is immobilized on the collagen surface and is distributed homogeneously. This is because the high molecular weight of the PMA causes the polymer to be located primarily on the surface of the collagen gel. When the PMA and collagen are premixed and gelled, the razor blade-cut surface shows that the porous and non-porous structures coexist (picture not shown). In the case of MiC-11 and MiC-12, the non-porous outer layer is very thin and the pore size is bigger, indicating that a sizeable amount of swelling had occurred.

3.2. Network structure of collagen gels

Shrinkage temperature T_s is considered as the rupture of the inter-chain bonds bringing the fusion of the oriented peptide chains [27], which is responsible for the shrinkage, and the cross-linking will result in the stabilization of the triple helix structure and an increase in the shrinkage temperature [28]. Table 2 lists T_s of the respective collagen gels. The result indicates that T_s would increase when the gels are cross-linked. Because PMA is immobilized, T_s of the gels would shift to a higher temperature, eventually reaching approximately 85 °C, which is about a 30 °C increase from that of uncross-linked collagen gel. The EN-1 gel and the MiC-11 and MiC-12 gels showed that T_s is lower than the EN-2 gel and the MiC-21 and MiC-22 gels. This implies that formation of inter- and intrahelical cross-links, which prevent the fusion of the peptide chains, is very important for stabilization of the network. The immobilization of PMA made the extra cross-link, that is, the bond between the PMA chain and collagen microfibril by the amide bond, eventually increasing T_s further. Comparing T_s of MiC-11 and MiC-12, we can see that the numeric value is almost the same. The same phenomenon can be seen for MiC-21 and MiC-22, implying that the immobilization of PMA would be affected by the pH of the MES buffer. Under pH 4.5, the carboxyl groups of PMA would be protonated, leading to the formation of COO–NHS, because the pK_a of PMA is known to be 2.7 [29].

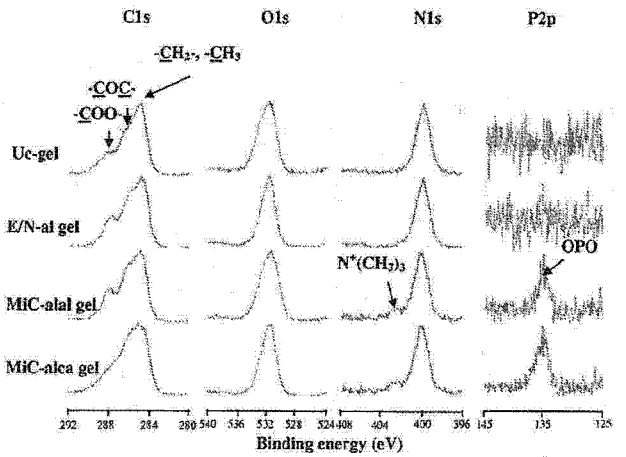

Fig. 3. XPS chart of Uc-gel, E/N-2l gel, MiC-22 gel, and MiC-21 gel. The takeoff angle of photoelectron was 90°.

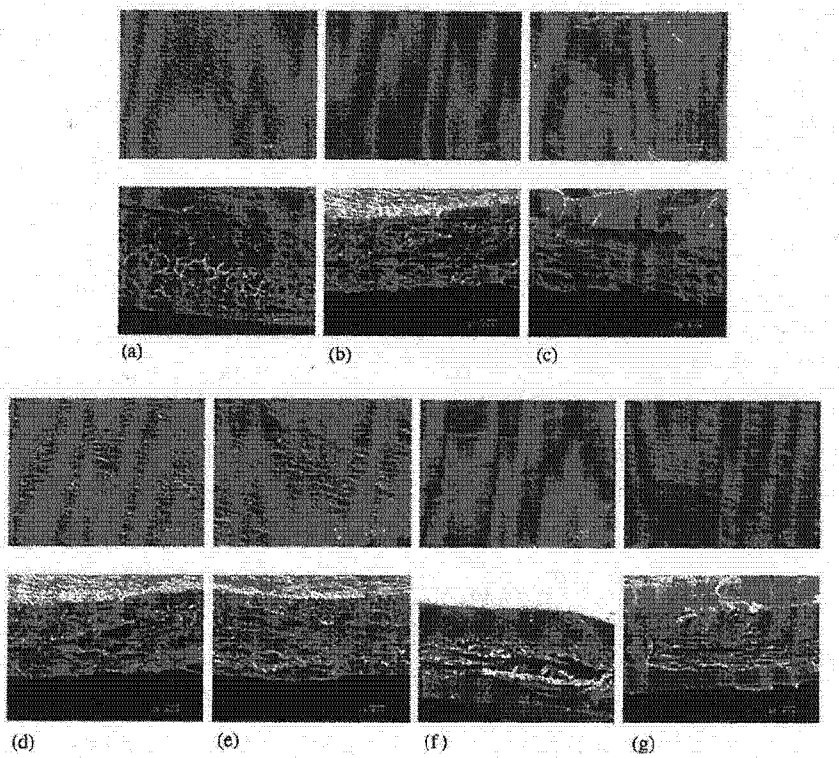

Fig. 4. Outer surface morphology (upper) and razor blade cut morphology (below) of respective gels: (a) Uc-gel, (b) E/N-1 gel, (c) E/N-2 gel, (d) MiC-11 gel, (e) MiC-12 gel, (f) MiC-22 gel, and (g) MiC-21 gel.

Table 2
Shrinkage temperatures of collagen and collagen gels

Sample	T_s (°C)
Uncross-linked	56.4±8.1
EN-1	67.4±0.9
EN-2	76.5±2.9
MiC-11	74.1±3.9
MiC-12	75.1±2.0
MiC-21	84.8±2.0
MiC-22	84.1±3.9

Fig. 5 shows the strain–stress curve of the Uc-gel, EN-2 gel, MiC-22, and MiC-21 gels. It can be seen that all collagen gels are J-shaped. This shape indicates that, after the cross-linking and immobilization processes, the collagen maintains its soft tissue viscoelastic behavior, which is soft and tough [30]. Table 3 shows the results of the elongational strain modulus of the respective gels at 1% and 8% of strain. Cross-linking with EDC/NHS increased the elongational strain modulus approximately five times and immobilization of PMA increased the elongational strain modulus about 12.5 times that of the uncross-linked collagen gel. The cross-linking process and immobilization of PMA made the collagen gel much tougher. This strongly suggests that the PMA must be immobilized onto the surface of the collagen gel in order to maintain its biomolecular property and stronger mechanical property

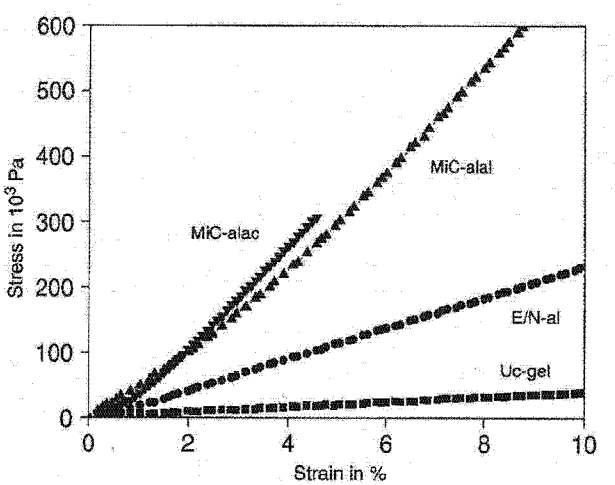

Fig. 5. Stress–strain curve of respective collagen gels.

simultaneously. The EN-1 gel, MiC-21, and MiC-11 gels were too fragile to measure the strain modulus.

Fig. 6 shows the swelling of the respective gels under pH 2.4 and pH 7.4. For uncross-linked gels, the gel dissolved under pH 2.4, while it swelled approximately 1400% under pH 7.4. When collagen gels absorb water, the triple helix structure is known to turn into a random coil conformation because the collagen peptide chains increase the accessibility to hydration. In the neutral and alkaline

Table 3
Mechanical strength of the collagen gels

Sample	Strain modulus at 1% (MPa)	Strain modulus at 8% (MPa)
Uncross-linked	0.4±0.1	0.6±0.1
EN-2 gel	2.1±0.1	2.9±0.2
MiC-21	5.6±1.1	8.7±1.6
MiC-21	5.1±0.6	8.0±1.0

Mechanical strength of EN-1, MiC-11 and MiC-12 was not measured due to fringe nature of the samples.

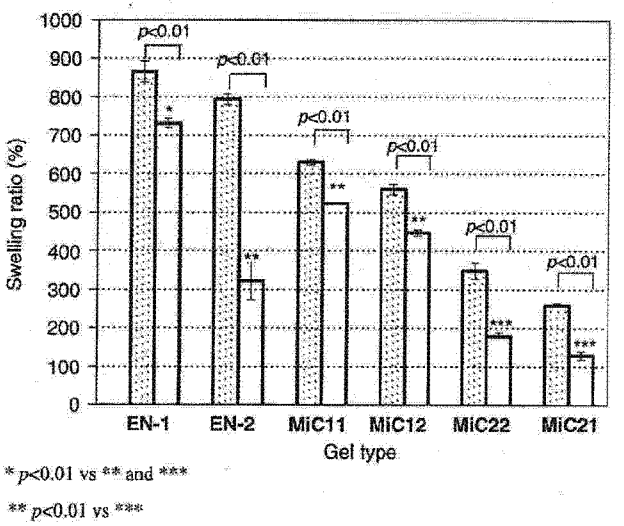

Fig. 6. Swelling ratio of respective collagen gels under pH 2.1 (hatched bar) and under pH 7.4 (empty bar) aqueous solutions. Each value represents the mean±SD ($n = 5$).

conditions, collagen film would be stabilized by forming an entanglement of fibrils formed by hydrophobic and electrostatic bonds [31–33]. Since the pK_a of collagen type I is known to be approximately 5.5 [34,35], a stable gel without any cross-linker can be formed under neutral and alkaline conditions.

The EN-1 and EN-2 gels showed a high swelling ratio under pH 2.1, but had different swelling ratios under neutral pH conditions. The EN-1 gels showed a swelling ratio of about 870% under pH 2.4 and 730% under pH 7.4, while the EN-2 gels showed 800% under pH 2.4 and 320% under pH 7.4. The swelling ratio was relatively higher for the EN-1 gel than the EN-2 gel because the network density was much higher for the EN-2 gel. The EN-2 gel, for which cross-linking was executed under alkaline conditions, is thought to possess a denser cross-linking network. As mentioned earlier, EDC and NHS are known to bring inter- and intrahelical cross-links, holding the α-helices together tightly. [36,37].

Immobilization of PMA on the collagen gels brought different swelling ratios according to the conditions of preparation. For the MiC-11 and MiC-12 gels, the swelling ratio was lower than that for the EN-1 gel, implying that a network between collagen and PMA is formed by the interchain cross-links. However, their swelling ratio under pH 2.4 was lower than that for the EN-2 gel, but was higher under pH 7.4. PMA could not penetrate into the collagen gel during the immobilization process, leaving much of the amine groups unreacted. In contrast, MiC-21 and MiC-22 showed that the swelling ratio under pH 2.4 and pH 7.4 would be lowest among all collagen gels. As mentioned earlier, the formation of a denser network brought a lower swelling ratio. The low swelling ratio of the MiC-11 and MiC-12 gels under pH 2.4 and pH 7.4 implies that the intra- and interhelical cross-links play important roles in the stabilization of the collagen gels.

3.3. Degradation of collagen gels by collagenase

Fig. 7 shows the degradation of collagen gels caused by the activation of collagenase in Tris-HCl buffer. The collagenase absorbed into the collagen gel would cleave the helical segment, hydrolyzing the collagen gels. Collagenase is known to be adsorbed onto the collagen fibers once it penetrates into the fiber [36–39]. Therefore, it is thought that the swelling ratio is related to this biodegradation process.

Our study shows that the collagen gel that is not cross-linked would degrade within 2 or 3 h. Cross-linking the collagen with EDC and NHS would strongly maintain the helical structure, extending the time of complete degradation from 6 to 24 h according to the cross-linking conditions. Low swelling collagen gels lead to slow degradation. For the MiC-22 and MiC-21 gels, almost 80% of the original collagen gel remained after 24 h. The E/N gels have only intra- and interhelical cross-links while the MiC gels possess interchain cross-links. For the E/N

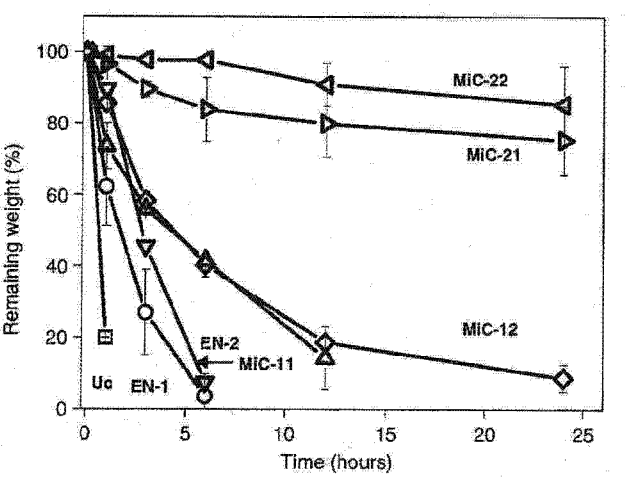

Fig. 7. Degradation of collagen gels by collagenase in Tris-HCl buffer (pH 7.4) at 37 °C. Each value represents the mean±SD ($n = 4$).

gels, the intra- and interhelical cross-links maintained the helical structure after cleavage by collagenase [39]. However, the absorption of water eventually made the E/N gels dissociate within 24 h, with slightly faster degradation for the EN-1 gel. In contrast, the MiC gels possess interchain cross-links that link the microfibrils and the PMA chains, making the degree of swelling much lower [38]. The cleavage by collagenase would be prevented by the PMA-collagen network, which links microfibrils together, shielding the helices.

4. Conclusion

We were able to successfully immobilize MPC to collagen and prepare a stable gel. By using collagen film prepared from 0.5 wt% collagen solution, MiC gels were prepared under MES buffer. EDC/NHS and PMA polymer could form a cross-link with the collagen film. The physical behaviors of the gels changed according to the preparation conditions such as the pH of the MES buffer. Inter- and intrahelical cross-links were formed by EDC/NHS. Higher cross-link efficiency can be obtained under an alkaline condition because the pK_a of collagen is approximately 5.5. A pre-NHS activated PMA polymer chain could be located on the collagen gel and cross-linked with the amine collagen group, forming an interchain cross-link. Since the pK_a of PMA carboxyl groups is 2.7, the immobilization of PMA was successful at any pH. The coexistence of intra- and interhelical cross-links and intermolecular cross-links make the network much denser, which leads to difficulty in either penetration or hydrolyzation by the collagenase. Mechanical and enzyme stability enable this gel to be applied as a biosynthetic hybrid biomaterial.

We will report on the biological properties of the collagen–phospholipid polymer hybrid gel in the near future.

Acknowledgment

This study was financially supported by a grant from the Research on Health Sciences Focusing on Drug Innovation (KH61060) of the Japan Health Sciences Foundation and Health and Labour Sciences Research Grants (HLSRG).

We would like to thank Professor Kazuhiko Ishihara of The University of Tokyo for his helpful advice on phospholipid polymer.

References

[1] Fujioka K, Maeda M, Hojo T, Sano A. Protein release from collagen matrices. Adv Drug Deliv Rev 1998;31:247–66.
[2] Kato YP, Silver FH. Formation of continuous collagen fibers: evaluation of biocompatibility and mechanical properties. Biomaterials 1990;11:169–75.
[3] Olde Damink LHH, Dijkstra PJ, van Luyn MJA, van Wachem PB, Nieuwenhuis P, Feijen J. Crosslinking of dermal sheep collagen using a water-soluble carbodiimide. Biomaterials 1996;17:765–73.
[4] Cascone MG, Barbani N, Cristalli C, Giusti P, Ciardelli G, Lazzeri L. Bioartificial polymer materials based on polysaccharides. J Biomater Sci Polym Edn 2001;12:267–81.
[5] Barbani N, Lazzeri L, Cristalli C, Cascone MG, Polacco G, Pizzirani G. Bioartificial materials based on blends of collagen and poly(acrylic acid). J Appl Polym Sci 1999;72:971–6.
[6] Cascone MG, Martinti S, Barbani N, Laus M. Effect of chitosan and dextran on the properties of poly(vinyl alcohol) hydrogels. J Mater Sci Mater Med 1999;10:431–5.
[7] Sionkowska A. Interaction of collagen and poly(vinyl pyrrolidone) in blends. Eur Polym J 2003;39:2135–40.
[8] Dascălu MC, Vasile C, Silvestre C, Pascu M. On the compatibility of low density polyethylene/hydrolyzed collagen blends. II: new compatibilizers. Eur Polym J 2005;41:1391–402.
[9] Olde Damink LHH, Dijkstra PJ, van Luyn MJA, van Wachem PB, Nieuwenhuis P, Feijen J. Glutaraldehyde as a crosslinking agent for collagen-based biomaterials. J Mater Sci Mater Med 1995;6:460–72.
[10] Sung HW, Chang WH, Ma CY, Lee MH. Crosslinking of biological tissue using genipin and/or carbodiimide. J Biomed Mater Res 2003;64A:427–38.
[11] Orban JM, Wilson LB, Kofroth JA, El-Kurdi MS, Maul TM, Vorp DA. Crosslinking of collagen gels by transglutaminase. J Biomed Mater Res 2004;68:756–62.
[12] Segura T, Chung PH, Shea LD. DNA delivery from hyaluronic acid–collagen hydrogels via a substrate-mediated approach. Biomaterials 2005;26:1575–84.
[13] Wissink MJB, Beernink R, Pieper JS, Poot AA, Engbers GHM, Beugeling T, et al. Immobilization of heparin to EDC/NHS-crosslinked collagen, characterization and in vitro evaluation. Biomaterials 2001;22:151–63.
[14] Perper JS, Hafmans T, Veerkamp JH, van Kuppevelt TH. Development of tailoir-made collagen-glycosaminoglycan matrices: EDC/NHS crosslinking, and ultrastructural aspects. Biomaterials 2000;21:581–93.
[15] Jaworski J, Klapperich CM. Fibroblast remodeling activity at two- and three-dimensional collagen–glycosaminoglycan interfaces. Biomaterials 2006;23:4212–20.
[16] van Luyn MJA, van Wachem PB, Olde Damink LHH, Dijkstra PJ, Feijen J. Relations between in vitro cytotoxicity and crosslinked dermal sheep collagens. J Biomed Mater Res 1992;26:1091–110.
[17] van Wachem PB, van Luyn MJA, Olde Damink LHH, Dijkstra PJ, Nieuwenhuis P. Biocompatibility and tissue regenerating capacity of crosslinked dermal sheep collagen. J Biomed Mater Res 1994;17:353–63.
[18] van Wachem PB, Zeeman R, Dijkstra PJ, Feijen J, Hendriks M, Cahalan PT, et al. Characterization and biocompatibility of epoxy-crosslinked dermal sheep collagens. J Biomed Mater Res 1999;47:270–7.
[19] Ishihara K, Ueda T, Nakabayashi N. Preparation of phospholipid polymers and their properties as polymer hydrogel membranes. Polym J 1990;22:355–60.
[20] Iwasaki Y, Mikami A, Kurita K, Yui N, Ishihara K, Nakabayashi N. Reduction of surface-induced platelet activation on phospholipid polymer. J Biomed Mater Res 1997;36:508–15.
[21] Ishihara K, Nomura H, Mihara T, Kurita K, Iwasaki Y, Nakabayashi N. Why do phospholipid polymers reduce protein adsorption? J Biomed Mater Res 1998;39:323–30.
[22] Kitano H, Imai M, Mori T, Gemmei-Ide M, Yokoyama Y, Ishihara K. Structure of water in the vicinity of phospholipid analogue copolymers as studied by vibrational spectroscopy. Langmuir 2003;19:10260–6.
[23] Ueda H, Watanabe J, Konno T, Takai M, Saito A, Ishihara K. Asymmetrically functional surface properties on biocompatible phospholipid polymer membrane for bioartificial kidney. J Biomed Mater Res A 2006;77:19–27.

[24] Watanabe J, Ishihara K. Phosphorylcholine and poly(D,L-lactic acid) containing copolymers as substrates for cell adhesion. Artif Organs 2003;27:242–8.
[25] Olde Damink LHH, Dijkstra PJ, van Luyn MJA, van Wachem PB, Nieuwenhuis P, Feijen J. In vitro degradation of dermal sheep collagen crosslinked using a water-soluble carbodiimide. Biomaterials 1996;17:679–84.
[26] Nakajima N, Ikada Y. Mechanism of amide formation by carbodiimide for bioconjugation in aqueous media. Bioconjugate Chem 1995;6:123–30.
[27] Flory PJ, Garrett RR. Phase transitions in collagen and gelatin systems. J Am Chem Soc 1958;80:4836–45.
[28] Khor E, Li HC, Wee A. Animal tissue-polypyrrole hybrid biomaterials: shrinkage temperature evaluation. Biomaterials 1996;17:1877–9.
[29] Nam K, Watanabe J, Ishihara K. Modeling of swelling and dissociation mechanism, and release behavior of spontaneously forming hydrogel composed of phospholipid polymers for oral delivery carrier. Int J Pharma 2004;275:259–69.
[30] Gentleman E, Lay AN, Dickerson DA, Nauman EA, Livesay GA, Dee KA. Mechanical characterization of collagen fibers and scaffolds for tissue engineering. Biomaterials 2003;24:3805–13.
[31] Ripamonti A, Roveri N, Briga D. Effects of pH and ionic strength on the structure of collagen fibrils. Biopolymers 1980;19:965–75.
[32] Wallace D. The relative contribution of electrostatic interactions to stabilization of collagen fibrils. Biopolymers 1990;29:1015–26.
[33] Rosenblatt J, Devereux B, Wallace D. Dynamic rheological studies of hydrophobic interactions in injectable collagen biomaterials. J Appl Polym Sci 1993;50:953–63.
[34] Luescher M, Ruegg M, Schindler P. Effect of hydration upon the thermal stability of tropocollagen and its dependence on the presence of neutral salts. Biopolymers 1974;13: 2489–503.
[35] Zhang J, Senger B, Vautier D, Picart C, Schaaf P, Voegel J-C, et al. Natural polyeletrolyte films based on layer-by-layer deposition of collagen and hyaluronic acid. Biomaterials 2005;26: 3353–61.
[36] Zeeman R, Dijkstra PJ, van Wachem PB, van Luyn MJ, Hendriks M, Cahalan PT, et al. Successive epoxy and carbodiimide crosslinking of dermal sheep collagen. Biomaterials 1999;20:921–31.
[37] Vizárová K, Bakos D, Rehákova M, Petríkova M, Panáková E, Koller J. Modification of layered atelocollagen: enzymatic degradation and cytotoxicity evaluation. Biomaterials 1995;16: 1217–21.
[38] Park S-N, Park J-C, Kim HO, Song MJ, Suh H. Characterization of porous collagen/hyaluronic acid scaffold modified by 1-ethyl-3-(3-dimethylaminopropyl)carbodiimide cross-linking. Biomaterials 2002;23:1205–12.
[39] Ma L, Gao C, Mao Z, Zhou J, Shen J. Enhanced biological stability of collagen porous scaffolds by using amino acids as novel cross-linking bridges. Biomaterials 2004;25:2997–3004.

Transactions of the Materials Research Society of Japan 31[3] 735-738 (2006)

Influence of Cross-linking on Physicochemical and Biological Properties of Collagen-Phospholipid Polymer Hybrid Gel

Kwangwoo Nam, Tsuyoshi Kimura and Akio Kishida
Institute of Biomaterials and Bioengineering, Tokyo Medical and Dental University Kanda-Surugadai 2-3-10, Chiyoda-ku, Tokyo 101-0062, Japan.
FAX:81-3-5280-8029, e-mail: bloodnam.fm@tmd.ac.jp

To adopt collagen as a biomaterial, collagen should be modified due to disadvantages such as poor mechanical strength and high thrombogenicity. Preparation of collagen-polymer hybrid gel for application as an artificial vascular graft was executed by immobilizing 2-methacryloyloxyethyl phosphorylcholine (MPC) polymer, poly(MPC-*co*-methacrylic acid) (PMA), using *N*-(3-dimethylaminopropyl)-*N'*-ethylcarbodiimide and *N*-hydroxysuccinimide as cross-linkers. In order to alter the density of interchain cross-links (intermolecular bonding) between collagen fibrils and the MPC polymer chains, collagen-polymer hybrid gel was prepared by changing the mole ratio of MPC moiety of PMA. The intra- and interhelical cross-links made the gel thermodynamically stable. The interchain cross-links made the gel mechanically and dimensionally stable by supporting the network structure of the hybrid gel, which is thought to be achieved by connecting collagen fibrils. Enzymatic stability was depending on the density of interchain cross-links, because the adsorption of collagenase was prohibited. Increase in the MPC moiety made the gel cell adhesion property decrease. This implies that the interaction between cells and surface of the hybrid gel is being regulated by the MPC groups, making the hybrid gel much efficient for artificial vascular graft use.
Key words: collagen, phospholipids polymer, cross-link, gel, cell adhesion

1. INTRODUCTION

In order to use collagen for a biomaterial product, the cross-linking of collagen and/or immobilizing synthetic polymer with collagen to is indispensable. Non-treated natural collagen cannot directly be applied to the biological system due to disadvantages such as poor mechanical strength, calcium deposition, and high thrombogenicity. However, the collagen is biocompatible and non-antigenic, synergic with bioactive component, easily modifiable, and available in abundance, which makes it suitable for medical application [1-3]. While keeping the advantageous property of collagen, disadvantageous property should be eliminated or be complemented.

Cross-link method using *N*-(3-dimethyl-aminopropyl)-*N'*-ethylcarbodiimide (EDC) and *N*-hydroxysuccinimide (NHS) was chosen for this study [4,5]. Cross-linking collagen with EDC and NHS makes 'zero-length' amide cross-links between carboxylic acid groups from aspartic and glutamic acid residues, and ε-amino groups from (hydroxy-) lysine residues forming intra- and interhelical cross-link to prepare an EDC/NHS cross-link collagen gel [5]. And, 2-methacryloyloxyethyl phosphorylcholine (MPC) based copolymer, which is known for its excellent biocompatibility [6], was used to cross-link the microfibrils of collagen to produce a hybrid gel having biocompatibility and improved mechanical strength.

In this study, we investigated the network structure of the collagen-phospholipid polymer hybrid gel and the effect to the mechanical strength, thermal stability, dimensional stability, and enzymatic stability against collagenase. Furthermore, the biological property of the collagen gel was examined to evaluate the application as an artificial blood vessel.

2. EXPERIMENTAL

2.1 Preparation of EDC and NHS Cross-linked Collagen Gel

Preparation of EDC and NHS cross-linked collagen gel (E/N gel) was executed by using 0.5wt% collagen type I solution (pH 3, KOKEN, Tokyo, Japan). Collagen solution was fabricated into film. Then the collagen film was immersed into the 0.05M 2-morpholinoethane sulfonic acid (MES) buffer (pH 9) (Sigma, St Louis, USA) containing EDC (Kanto Chemicals, Tokyo, Japan) and NHS (Kanto Chemicals, Tokyo, Japan). The cross-linking procedure was executed for 4 hours at 4°C to make a cross-linked gel (E/N-al gel). After 4 hours, the reaction was stopped and the gel was then washed with 4M of Na_2HPO_4 aqueous solution for 2 hours to hydrolyze any remaining *O*-acrylisourea groups and then with distilled water for 3 day to remove salt from the gel. The molar ratio of each chemical was fixed to EDC:NHS:collagen-carboxylic acid groups=5:5:1.

2.2 Preparation of MPC-immobilized Collagen gel

Preparation of the MPC-immobilized Collagen gel (MiC gel) was executed by using E/N-al gel. poly(MPC-*co*-methacrylic acid) (mole ratio; MPC:methacrylic acid=3:7, PMA30) (Figure 1) was added with EDC and NHS in MES buffer (pH 10) and was pre-activated for 10 minutes before E/N-al gel was immersed. The molar ratio of each chemical was fixed to EDC:NHS:carboxylic acid groups of PMA =5:5:1. The immobilization of PMA to the collagen was continued for 4 hours at 4°C. Then the gel was washed with 4M of Na_2HPO_4 aqueous solution for 2 hours and then with distilled water for 1 day to remove salt from the gel to prepare a salt-free MiC30 gel. To increase the MPC moiety of the collagen-polymer hybrid gel, PMA90 (MPC:methacrylic acid=9:1) was prepared and immobilized to the collagen to make a MiC90 gel.

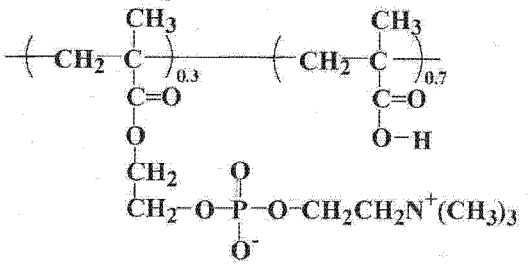

Figure 1.Chemical structure of PMA.

2.3 Surface Characterization

The surface analysis was executed using X-ray photoelectron spectroscopy (XPS; AXIS-HSi, Shimadzu/KRATOS, Kyoto, Japan) and Scanning electron microscopy (SEM; SM-200, Topcon, Tokyo, Japan) Samples which had been cut into small pieces were lyophilized for overnight. The chemical composition of the surfaces of the gel (upper part of the gel) was determined by releasing angle of the photoelectrons fixed at 90°. The morphologies of the gels were observed with a SEM. The razor-blade cut surfaces of respective gels were observed.

2.4 Network Characterization

The shrinkage temperature of the gels were determined using differential scanning calorimeter (DSC; DSC6000, Seiko, Chiba, Japan) in the range of 0°C to 150°C at the scanning rate of 5°C/minute.

Stress-strain curves of respective collagen gels were determined by uniaxial measurements using a tensile strength tester (STA-1150, Orientec, Tokyo, Japan). The sample for the measurement was prepared in the size of 4cm×1cm. The obtained data were changed to stress-strain curve of the samples and the elongation modulus was calculated.

The swelling test of respective samples was executed by cutting lyophilized gels into small pieces and putting into pH aqueous solution at 37°C. The pH of the aqueous solution was controlled to make 7.4. The gels were shaken gently for 24 hours and taken out to measure the changed weight of the sample. Swelling ratio was calculated in order to define the exact swelling phenomenon brought up by water absorption.

2.5 Enzymatic Degradation

The degradation test of the gel samples were executed using collagenase from Clostridiopeptidase histoluticum (EC 3.4.24.3, *Sigma*, St Louis, USA) with collagenase activity of 320 units/mg. In this experiment, collagen gels were immersed into Tris-HCl buffer solution with total concentration of collagenase 100units/mL. The weight of the gels after reaction with collagenase was measured from 1 to 72 hours.

2.6 Cell adhesion test

L-929 cells (mouse fibroblast) were used to evaluate the interaction between collagen gels and the cells. The fibroblasts were culture in Eagle's Minimum Essential Medium (E-MEM; Gibco, NY, USA) supplemented with 10% fetal bovine serum (FBS; Gibco, NY, USA) at 37°C in a 5% CO_2 atmosphere. After treatment with 0.25% trypsin, the cell density was adjusted to 5×10^3 cells/mL and the cells were seeded on the surface. The collagen gels were sterilized by putting gels into ethanol:water 50:50 for 2 hours, than 70:30 for 2 hours, and 100:0 for an overnight before lyophilizing. The lyophilized gels were hydrolyzed with E-MEM for 5 minutes and the E-MEM was disposed just before cell seeding. After 24 hours and 48 hours, the number of adhering cells was determined using lactate dehydrogenase (LDH) assay at 560nm with UV/VIS spectrophotometer (V-560, Jasco, Tokyo, Japan).

3. RESULTS AND DICUSSION

3.1 Surface Characterization

All gels showed XPS signals attributed to carbon in CH_3- or $-CH_2$-, -COC-, C(=O)-, and nitrogen in -CONH- was observed at 285, 286.6, 288.5, and 400.8eV, respectively. A phosphorus peak and one nitrogen peak in $-N^+(CH_3)_3$ was observed at 134eV and 403.2eV, respectively, indicating that PMA was properly cross-linked collagen [6]. Figure 2 shows the images of the outer surface (upper part of the gel) and razor blade-cut surface (cross-section) morphology of respective collagen gels observed with SEM. All outer surfaces that are immobilized with PMA show non-porous homogenous structure. When the razor-cut surface was observed, relatively porous (or hollow) layer that is composed of many thin plates, and non-porous (or dense) layer was seen. Hollow layer is thought be the uncross-linked collagen (a collagen gel that is prepared under pH 9.0 MES buffer without any cross-linker; Uc gel) or intra- and interhelically cross-linked collagen layer. The non-porous layer representing PMA is deposited on the collagen layer and the thickness increases as more PMA is adopted. However, we are not sure yet how the deposited layer would affect the physical property of the hydrogel. We are working on this and would be reported soon.

3.2 Network Characterization

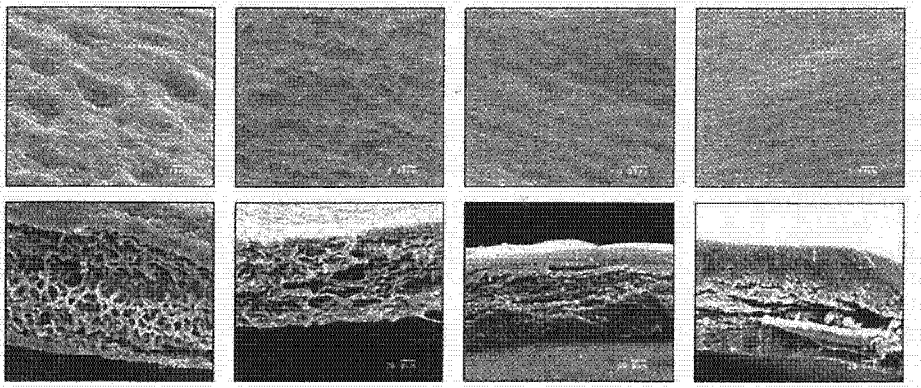

Figure 2. SEM images of collagen gels. (a) Uc gel, (b) E/N gel, (c) MiC90 gel, and (d) MiC30 gels. Upper images imply the outer surface and below images indicate the razor-cut surface of the gels.

Table I shows the change of the shrinkage temperature (T_s) of each collagen gels. The cross-linking brought the increase in the T_s. And the T_s would increase further as the PMA is immobilized, but would never cross 85°C. Since the denaturization temperature is the endothermic transition of the triple helix of the collagen molecules to the random coil, it is believed that intra- and interhelical cross-link controls the T_s [7]. When the higher amount of EDC and NHS was used, the T_s would increase up to 83°C (data not shown). This implies that the increase in the T_s is not due direct connection between collagen microfibrils and polymer chain but due to complexity of the network. So, the stability of the collagen gels against temperature is dependant not only on intra- and interhelical cross-links, but also on the density of the network.

Table I. Shrinkage temperature of respective collagen gels.

Sample	Shrinkage temperature (°C)
Uc gel	56±8
E/N gel	74±3
MiC90	76±3
MiC30	84±4

The elongational modulus increases as PMA is immobilized, indicating it is the interchain cross-link that reinforces the mechanical strength. The elongational modulus of MiC gels measured at 1% strain and 8% strain showed that approximately 10~13 times increase compared to Uc-gel while that of E/N gel showed approximately 5 times increase. This indicates that the network is much denser for MiC gels, which directly affected the mechanical strength.

All collagen gels showed 1.4~2 times increase in elongational modulus at 8% strain compared to that of at 1% strain, indicating soft tissue viscoelastic behavior can be maintained after immobilizing with PMA. So, biomaterial possessing biological property can be obtained.

Figure 3 shows the swelling of the respective gels under pH 7.4. For uncross-linked gel, the gel dissolved under pH 2.1, while swelled approximately 1400% under pH 7.4. When collagen gels absorb water, the triple helix structure is known to turns to random coil conformation, because collagen peptide chains increases accessibility to hydration. In the neutral and alkaline pH conditions, collagen film would be stabilized by forming entanglement of fibrils formed by hydrophobic and electrostatic bonds.

E/N-al gels shows swelling ratio of 320% under pH 7.4. As mentioned earlier, EDC and NHS is known to be bring inter- and intrahelical cross-links, holding the α-helices together tightly. However, its low cross-linking density due to high free amine group contents makes the gel to swell high.

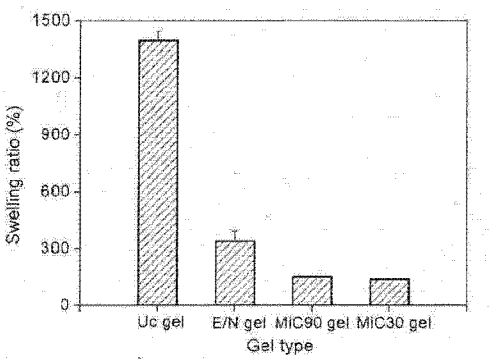

Figure 3. Swelling ratio of respective collagen gels in pH 7.4

MiC gels shows much suppressed swelling ratio. The decrease in the swelling ratio comparing to E/N gel indicates that the dense network has formed. Denser network between collagen and PMA is thought to be formed by interchain cross-links by connecting microfibrils together, increasing the toughness of the collagen gel. Furthermore, the high mechanical strength of the hybrid gel is suppressing the absorption of water, leading to low swelling ratio.

3.3 Enzymatic Degradation

Figure 4 shows the degradation of collagen gels caused by the activation of collagenase in Tris-HCl buffer. Collagen gel would be degraded once it encounter with collagenase. Collagenase would cleave the helical segment, which makes the collagen gels to hydrolyze. Collagenase is known to absorb onto the collagen fibers once it penetrates into the fiber [7]. Our study shows that the collagen gel that is not cross-linked would be degraded within 2 or 3 hours. Cross-linking the collagen with EDC and NHS would maintain the helical structure firmly, extending the complete degradation time from 3 hours to 24 hours. And as mentioned previously, the E/N-al gel possesses higher intra- and intercross-link chains, making the gel to endure longer time against collagenase.

MiC gels showed higher stability against collagenase. The network of the collagen gel is thought to be denser than E/N gel, as described previously. For E/N gels, the absorption of collagenase eventually made it to be dissociated within 24 hours. On the other hand, MiC gels possess interchain cross-link, which links the microfibrils and the PMA chains, making the gel to swell much lower. And the cleavage by collagenase would be prevented by the PMA-collagen network which links fiber and polymer chain together, shielding the helices

Comparing the degradation rate between MiC gels, we can see that as MPC ratio increases, the degradation is much faster. This is because the network of the MiC90 is thought to be much sparse than MiC30, due to low mole ratio of methacrylic acid moiety. This makes the space between collagen and PMA larger, resulting in higher water absorbance.

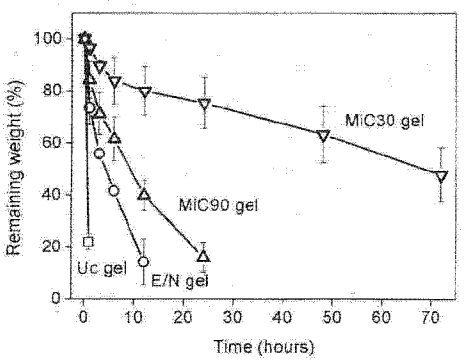

Figure 4. Degradation of collagen gels by collagenase in Tris-HCl buffer (pH 7.4) at 37°C.

3.4 Cell Adhesive property

When the number of adhered cells after 24 hours and 48 hours were compared among the collagen gels, and those with PMA immobilized on collagen gels were much lower than without PMA. This is clearly due to PMA polymer covering the surface of the collagen gel. The number of cell adhered on the surface decreased as the moiety of MPC unit increased. The difference between number of adhered cell on the surface after 24 and 48 hours was compared, the increase in the number of cells was observed for collagen gels. However, for MiC gels, increase was suppressed. Polymer immobilized on the collagen blocks the interaction between fibroblast and collagen, which is known to be the most decisive factor for cell adhesion [8].

4. CONCLUSION

The preparation of MiC gel was successfully achieved. Immobilization of MPC polymer made the gel tougher and stable. We could confirm that the stress-strain responded as generally observed for soft biological materials. Increase in the MPC unit brought the higher swelling, which lead to the faster degradation by collagenase. It is thought that the higher amount of adopted PMA have caused the formation of sparse cross-link network, which in turn make the surface of the MiC gel full of MPC head groups, reducing cell adhesion ability.

The increase in the MPC unit would bring higher biocompatilibty, while increase of MA unit would allow increment of mechanical strength. As the concentration of MPC increased, it is thought that the biocompatibility would increase but toughness decrease.

ACKNOWLEDGEMENT

This study was financially supported by Grant from the research on Health Science focusing on Drug Innovation (KH61060) of the Japan Health Sciences Foundation and Health and Labour Sciences Research Grants.

REFERENCES

[1] W. Friess, *Eur. J. Pharm. Biopharm.*, **45**, 112-136 (1998).
[2] K. Fujioka, M. Maeda, T. Hojo, and A. Sano, *Adv. Drug Del. Rev.*, **31**, 247-266 (1998).
[3] C.H. Lee, A. Singla, and Y. Lee, *Int. J. Pharma.*, **221**, 1-22 (2001).
[4] L.H.H. Olde Damink, P.J. Dijkstra, M.J.A. van Luyn, P.B. van Wachem, P. Nieuwenhuis, and J. Feijen, *Biomaterials*,**17**, 765-773 (1996).
[5] M.J.B. Wissink, R. Beernink, J.S. Pieper, A.A. Poot, G.H.M. Engbers, T. Beugeling, W.G. van Aken, and J. Feijen, *Biomaterials*, **22**, 151-163 (2001).
[6] K. Ishihara, T. Ueda, and N. Nakabayashi, *Polym. J.*, **22**, 355–360 (1990).
[7] R. Zeeman, P.J. Dijkstra, P.B. van Wachem, M.J. van Luyn, M. Hendriks, P.T. Cahalan, and J. Feijen, *Biomaterials*,**20**, 921-931 (1999).
[8] J. Watanabe and K. Ishihara, *Artif Organs*, **27**, 242-248 (2003).

(Received January 31, 2006:Accepted June 2, 2006)

systemic administration. This is achieved with a hydrophilic polymer of which polyethylene glycol (PEG) has been found to be best. Targeting cell-surface receptors is an attractive concept to achieve specific binding and internalisation of the liposome. To this end, cell-binding ligands are displayed from the surface of the liposome. The common denominator for these ligands is that their cell receptor targets are over-expressed in tumours.

We are developing a post-modification methodology for coupling cell or tissue targeting moieties onto liposomes via chemioselective oxime bond formation. Thus, liposomes comprising a highly nucleophilic aminoxy-functionalised lipid are formulated. The aminoxy lipid readily reacts with aldehyde functionalised targeting ligands in aqueous conditions forming a stable oxime bond conjugated targeted liposome.

A peptide displaying the RGD sequence was selected as the targeting ligands to validate our post-coupling methodology. A cyclic RGD peptide conjugate has been successfully synthesised using a combination of solution- and solid-phase synthesis. Additionally, control RGE peptide and PEG linker conjugates have been prepared. All the ligands terminate in an aldehyde functional group separated from the targeting moiety by a PEG linker.

The couplings between the RGD conjugate and aminoxy liposomes in water at pH ~4 were shown to be efficient, simple and reproducible. In vitro HUVEC cell uptake studies show a definite targeted uptake of the RGD-targeted liposomes relative to appropriate control liposomes.

193. Gene Transfection Using Inorganic Particle/PVA/DNA Complexes Prepared by Ultra High Pressure Technology

Tsuyoshi Kimura,[1] Kwangoo Nam,[1] Sihngo Mutsuo,[2] Hidekazu Yoshizawa,[2] Masahiro Okada,[3] Tsutomu Furuzono,[3] Toshiya Fujisato,[4] Akio Kishida.[1]

[1]Institute of Biomaterials and Bioengineering, Tokyo Medical and Dental University, Tokyo, Japan; [2]Department of Environmental Chemistry and Materials, Okayama University, Okayama, Japan; [3]Department of Biomedical Engineering, National Cardiovasucular Center Research Institute, Osaka, Japan; [4]Department of Regenerative Medicine and Tissue Engineering, National Cardiovasucular Center Research Institute, Osaka, Japan.

Various non-viral gene systems, such as naked DNA, lipoplexes, micelles and polyplexes, have been developed for effective and safe gene delivery into target cells. Although cationic compounds were employed as gene carriers due to the ability of complex formation with DNA electrostatically and effective gene transfer into cells, the intrinsic cytotoxicity of them is essential problem in non-viral gene delivery system. Therefore, we have tried the development of DNA complex with non-ionic, water soluble polymers via hydrogen bond using ultra high pressure (UHP) technology because the inter-, intra-molecular week hydrogen bonding interaction was empathized with high pressure process. Previously, polyvinyl alcohol (PVA) was utilized as the model hydrogen bonding polymers, and the PVA/DNA complexes were obtained by UHP treatment. Although the PVA/DNA complexes were up-taken by cells, a little enhancement of gene expression was observed using them. In this study, we hypothesize that inorganic particles, such as calcium phosphate (CP), calcium carbonate and hydroxy apatite (HAp), promote the endosomal escape of transferred DNA because the inorganic particles are dissolved under low pH condition in endosome vesicles and then the rupture of endosome is induced by osmotic shock. We performed the development of inorganic particle/PVA/DNA complexes using UHP technology. Plasmid DNAs encoding enhanced green fluorescent protein (EGFP) gene or luciferase gene under CMV promoter were used. Nano-HAps having the average diameter of 50nm were synthesized by modified micro-emulsion method. Nano-HAp was dispersed ultrasonically in PVA solution and then mixed with DNA solution. CP/DNA complexes were prepared by general method and mixed with PVA solution. Their mixtures were treated under 10000 atmospheric pressures at 40 degree for 10min. By SEM observation, the irregular surface of inorganic particles/PVA/DNA complexes was observed, indicating the encapsulation of inorganic particles in PVA/DNA particle. The nano-HAp/PVA/DNA complexes showed a higher transfection activity than DNA complexes with nano-HAp or PVA. With CP/PVA/DNA complexes, also, the transfection activity increased several fold than the PVA/DNA complexes. These results indicate the utility of the inorganic particle/PVA/DNA complexes prepared by the UHP treatment for DNA delivery.

194. Development of Novel DNA Formulations Based on Polymers and Cyclodextrin for Gene Delivery to the Muscle

Caroline Roques,[1,2] André Salmon,[1] Marc Y. Fiszman,[1] Elias Fattal,[2] Yves Frome.[1]

[1]Gene Therapy Lab, Institut de Myologie - INSERM u582, Paris, France; [2]CNRS UMR 8612, University of Paris - Faculty of Pharmacy, Chathenay-Malabry, France.

So far gene transfer to the muscle has mainly been based on viral vectors, given their efficiency to transfer DNA in vivo. However, virus-derived vectors have numbers of limitations, such as insert size, tissue specificity or immunogenicity, therefore restricting the possibilities of repeated administrations. After intramuscular injection, major hurdles remain tissue diffusion and intracellular entry.

To improve these parameters with reference to naked DNA, our approach consisted in designing synthetic vectors. The first step intended to condense and protect plasmid DNA (pCMV-βGal, Invitrogen) through its association with various polymers differing by their charge, i.e. Polyethyleneimine (PEI, Sigma), Tetronic 304 (BASF) and PE6400 (BASF). For each polymer/DNA formulation, the morphological properties of the vectors were assessed by cryo-Transmission Electron Microscopy, their size by Dynamic Light Scattering and their zeta potential by Laser Doppler Velocimetry. Characterization revealed a great diversity of objects in terms of size, shape and zeta potential.

In vivo toxicity and efficiency of the systems were also evaluated after intramuscular injections into tibialis anterior and quadriceps muscles of wild type Syrian hamsters. X-Gal revelation and Haematein/Eosin staining were then performed on serial sections of each muscle. These experiments highlighted the extremely high cytotoxicity of PEI/DNA complexes towards skeletal muscle. On the contrary, no significant lesions were detected after injection of PE6400/DNA or Tetronic/DNA formulations. Both systems did significantly improve transfection with reference to naked DNA.

In order to promote cellular entry of the DNA, a second step in our study consisted in combining the previous polymeric vectors with randomly methylated beta-cyclodextrin (Rameb) since this compound has demonstrated its ability to destabilize the cell membrane through cholesterol complexation. In vivo toxicity of Rameb after intramuscular injection has been assessed as well as efficiency when associated to polymer/DNA formulations. Addition of Rameb to the polymeric vectors did not allow a significant increase

Copyright © The American Society of Gene Therapy

Optimization of amino group density on surfaces of titanium dioxide nanoparticles covalently bonded to a silicone substrate for antibacterial and cell adhesion activities

Masahiro Okada,[1] Shoji Yasuda,[1] Tsuyoshi Kimura,[1] Mitsunobu Iwasaki,[2] Seishiro Ito,[2] Akio Kishida,[1] Tsutomu Furuzono[1]

[1]*Department of Bioengineering, National Cardiovascular Center Research Institute, 5-7-1 Fujishirodai, Suita, Osaka 565-8565, Japan*

[2]*Department of Applied Chemistry, Faculty of Science and Engineering, Kinki University, 3-4-1 Kowakae, Higashiosaka, Osaka 577-8502, Japan*

Received 7 April 2005; revised 14 June 2005; accepted 20 June 2005
Published online 1 September 2005 in Wiley InterScience (www.interscience.wiley.com). DOI: 10.1002/jbm.a.30513

Abstract: A composite consisting of titanium dioxide (TiO_2) particle, the surface of which was modified with amino groups, and a silicone substrate through covalent bonding at their interface was developed, and antibacterial and cell adhesion activities of the composite were evaluated. The density of the amino groups on the TiO_2 particle surface was controlled by the reaction time of the modification reaction. The degradation rate of CH_3CHO in the presence of the TiO_2 particles under UV irradiation decreased with an increase in the amino group density on the TiO_2 surface. On the other hand, the number of L929 cells adhering on the TiO_2/silicone composite increased with an increase in the amino group density. From the above two results, the optimum density of amino groups for both photoreactivity and cell adhesiveness was estimated to be 2.0–4.0 molecules/nm^2. The optimum amino group-modified TiO_2/silicone composite sheet (amino group density, 3.0 molecules/nm^2) showed an effective antibacterial activity for *Escherichia coli* bacteria under UV irradiation. © 2005 Wiley Periodicals, Inc. J Biomed Mater Res 76A: 95–101, 2006

Key words: titanium dioxide; antibacterial activity; composite; covalent bonding; cell adhesion

INTRODUCTION

Since Fujishima et al.[1] reported water cleavage on photoexcited titanium dioxide (TiO_2) electrodes, TiO_2 has attracted great interest in environmental fields such as air and water purification, because the electron and hole created by photoexcitation of TiO_2 can reduce or oxidize several chemical species adsorbed on the TiO_2 surface.[2–5] The antibacterial activity or cytotoxicity, which is expected to be applicable to biology and medicine, of photoexcited TiO_2 has also been shown.[6–8] In addition, the effect of TiO_2 particles on animals has been investigated from the viewpoint of genetic toxicity; Bischoff et al.[9] and Bernard et al.[10] reported the nontoxicity of TiO_2 particles to animals. TiO_2 has, therefore, also attracted much interest in medical fields.

Recently, we developed a novel inorganic/organic nanocomposite for a percutaneous device: a flexible silicone elastomer, the surface of which was modified with bioactive hydroxyapatite (HAp) nanoparticles through covalent bonding.[11] When this novel composite material is percutaneously implanted into a living body, it is expected to prevent initial germ infection from the outside because the HAp particles existing on the surface of the composite improve adhesion between living tissues and the composite. Actually, the novel composite showed good tissue adhesiveness in animal implant tests.[12] Furthermore, in a previous article,[13] we tried to incorporate two functions, that is, bioactivity and photoreactivity, into a percutaneous device by using TiO_2 particles. Such a system is expected to prevent damage by the antibacterial activity of photoexcited TiO_2 when a germ infection unfortunately occurs after implantation. In order to make covalent linkage between TiO_2 particles and a silicone

Correspondence to: T. Furuzono; e-mail: furuzono@ri.ncvc.go.jp

Contract grant sponsor: New Energy and Industrial Technology Development Organization (NEDO), Japan

© 2005 Wiley Periodicals, Inc.

substrate and to promote cell adhesion on TiO_2 particles, the surfaces of TiO_2 particles were modified with an amino group-terminated silane coupling agent. Although the composite showed good cell adhesiveness, the photoreactivity was approximately 30 times lower than that of the original TiO_2, which should be due to high coverage of the TiO_2 surface by amino groups.

In this article, in order to develop a TiO_2/silicone composite having both antibacterial and cell adhesion activities, the amino group density on the TiO_2 particle surface was optimized. Antibacterial activity test of the composite was additionally conducted in order to evaluate the functionality of the amino group-modified TiO_2/silicone composite.

MATERIALS AND METHODS

Materials

Anatase TiO_2 particles with an inter-diameter of 200–300 nm and a specific surface area of 5.0 m^2/g were kindly donated by Ishihara Sangyo Co., Ltd. (Osaka, Japan). A silicone sheet (Shin-Etsu Polymer Co., Tokyo, Japan) with a thickness of 0.3 mm was purified by methanol with a Soxhlet extractor. Acrylic acid (AAc; Nacalai Tesque, Inc., Kyoto, Japan) was purified by vacuum distillation. γ-Aminopropyltriethoxysilane (γ-APS; Shin-Etsu Chemical Industries Co., Tokyo, Japan) was used without further purification.

Introduction of amino groups on the surfaces of the TiO_2 particles

TiO_2 particles, 5.0 g, after drying at 120°C for 24 h were added to 150 mL of anhydrous toluene in a 300-mL three-necked flask equipped with an inlet of N_2, a reflux condenser, and a half-moon type stirrer. After the temperature of the mixture was raised to 30°C, γ-APS was injected into the mixture, and it was stirred at 30°C for different reaction periods. After the reactions, the TiO_2 particles were washed with toluene and acetone by centrifugation to remove any unreacted silane coupling agent and dried at 60°C for 24 h. The density of amino groups on the surfaces of the TiO_2 was calculated from the specific surface area of the particles and the weight percentage of carbon atoms in the modified particles. The weight percentage of carbon atoms was measured with an elemental analyzer (EMIA-110; Horiba Ltd., Kyoto, Japan), assuming that all of the amino groups existed on the particle surfaces.

Photoreactivity of the amino group-modified TiO_2 particles

The photoreactivity of the amino group-modified TiO_2 was evaluated by the degradation rate of CH_3CHO. The initial concentration of CH_3CHO in a Pyrex reaction vessel (760 mL) was fixed at approximately 300 ppm in air. UV/Vis light (wavelength, >300 nm) was irradiated with a Xe lamp (HX-500; Wacom Electric Co., Ltd, Tokyo, Japan) at 2000 $\mu W/cm^2$ onto the samples (0.07 g) after the adsorption equilibrium of CH_3CHO in the reaction vessel had been achieved. The concentration of CH_3CHO was determined by a gas chromatograph (GC-8APT; Shimadzu Co., Kyoto, Japan) equipped with an f.i.d. column Shincarbon A. The rate constant for the degradation of CH_3CHO was calculated from the first-order rate equation.[14,15]

TiO_2/silicone composite

First, graft-polymerization of AAc was conducted on the surface of the silicone sheet.[11] The silicone sheet was initially treated by corona-discharge to donate radicals on the surface. The sheet was immersed into a 10 wt% AAc aqueous solution in 50-mL thick-walled tubes, and the tubes were subsequently degassed and sealed. Polymerization was conducted at 60°C for 30 min, and the poly(AAc)-grafted silicone sheet was rinsed with a great deal of hot water to remove homopolymers adsorbed physically. Surface-treated sheets possessing a poly(AAc)-grafted density of 10–20 $\mu g/cm^2$ were used in this study.

In order to adsorb the modified TiO_2 particles onto the poly(AAc)-grafted silicone sheet, 0.2 g of the particles were suspended in 50 mL of water, and the sheet was soaked in the suspension for 1 h at room temperature. After the adsorption, the sheet was heated at 180°C for 2 h in a vacuum for a reaction between the amino groups on the TiO_2 particles and the carboxyl groups on the poly(AAc)-grafted silicone sheet. The composite was washed by using an ultrasonic generator for 3 min (output, 20 kHz; 35 W) in water to remove the particles physically adsorbed on the sheet. In the case of the original TiO_2 particles, the ultrasonic cleaning was not conducted because all of the particles were just physically adsorbed on the sheet. The surface of the composite was observed by scanning electron microscopy (SEM; JSM-6301F, JEOL Ltd., Tokyo, Japan), and the surface-coverage ratio by TiO_2 particles was determined from SEM images. In following experiments, the TiO_2/silicone composite sheets, whose surface-coverage ratio by TiO_2 particles were 50–60%, were used (Fig.1).

Cell adhesion

L929 mouse fibroblast cells were placed onto the TiO_2/silicone composite in 24-well multiplates at 1×10^5 cells/well in a culture medium consisting of an α-minimum essential medium (α-MEM; Gibco Laboratories Inc.) and 10% fetal bovine serum, and incubated at 37°C for 24 h. For SEM observation, the cells were dehydrated with aqueous ethanol (30–100%) and 100% *n*-butanol for 5 min at room temperature step by step. The samples were subsequently lyophilized and coated with gold. The number of L929 cells on the sample substrate was counted from SEM images. As a control sample, the poly(AAc)-grafted-silicone sheet, on

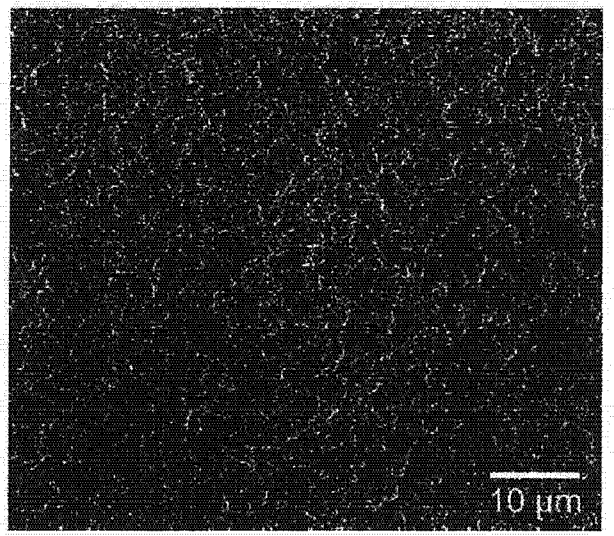

Figure 1. A typical SEM photograph of a surface of amino-group-modified TiO_2/silicone composite sheet, showing a 60% covered surface by the modified TiO_2 particles (amino group density, 3.0 molecules/nm^2).

which the original TiO_2 particles were physically adsorbed, was used.

Cytotoxicity assay

A cytotoxicity assay for the TiO_2/silicone composite was conducted as follows. One gram of the composite was cut into small pieces and added into 10 mL of cell culture medium (α-MEM with 10% fetal bovine serum), and the mixture was incubated at 37°C for 24 h in darkness. After L929 cells (initial number, 1×10^4 cells/well) were precultured at 37°C for 24 h, the culture medium was replaced by the medium exposed to the samples, and the cells were further incubated for another 24 h at 37°C. The number of cells was counted with a hemacytometer after trypsinization and dilution. As a control, the same procedure was conducted with a nontreated medium.

Antibacterial activity

E. coli bacteria (NBRC 3301 strain; Biological Resource Center, Biotechnology Center, National Institute of Technology and Evaluation, Chiba, Japan), precultured at 37°C for 16 h, were washed by centrifuging at 4000 rpm, resuspended, and diluted to 1×10^5 cells/mL with a physiological salt solution. The composite sheets were placed in 24-well multiplates, and then 1 mL of the *E. coli* suspension was pipetted into each well. This system was irradiated with a 4-W back-light bulb (wavelength, 360 nm; 470 μW/cm^2; FL15 BL-B; National Panasonic) at 37°C for 2 h. After the irradiation, 100 μL of each *E. coli* suspension was pipetted out and incubated in a nutrient agar medium at 37°C for 16 h, and the number of viable bacteria was counted. As a control test, the above procedure was conducted without the composite sheet or without UV irradiation.

Statistical analysis

Data resulting from cytotoxicity assays and antibacterial activity tests are presented as means ± SD for mean ($N = 4$). Statistical comparisons were performed with the use of a Student's t test. The level of statistical significance was defined as $p < 0.05$.

RESULTS AND DISCUSSION

The TiO_2 particles were chemically modified with an amino group-terminated silane coupling agent at 30°C for different reaction time. In the previous article,[13] modification with amino groups was confirmed by FT-IR. Figure 2 shows the density of amino groups on the surfaces of the TiO_2 particles after modification at 30°C for different reaction times. The density of the amino groups was determined from the specific surface area of the TiO_2 particles and the carbon content measured by elemental analysis. In order to determine the amino group density, the nitrogen content was not used because it was below the detection limit. The density of the amino groups incorporated on the particle surfaces drastically increased within 1 h, gradually increased with an increase in the reaction time, and then almost reached a plateau at about 5 molecules/nm^2. Judging from the fact that the theoretical density of the OH groups on the anatase TiO_2 surface is 12–14 molecules/nm^2, which is estimated from lattice constant,[16] and that each silane coupling agent reacts with less than three OH groups, it is estimated

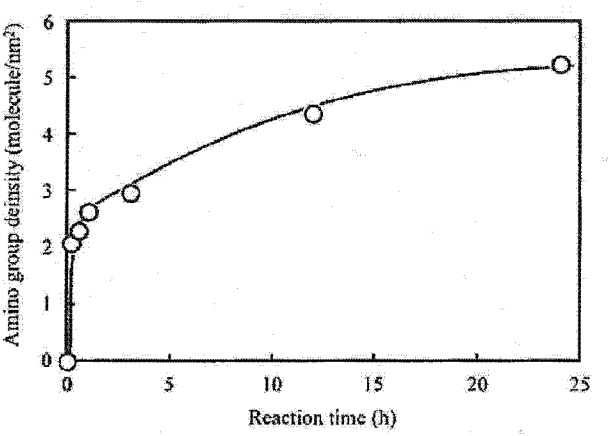

Figure 2. Amino group densities on the TiO_2 particle surfaces after modification at 30°C for different reaction times.

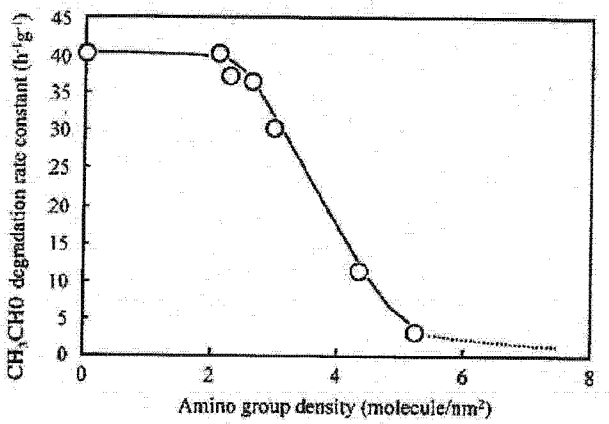

Figure 3. Relationship between the amino group density on the TiO_2 particle surfaces and the degradation rate constant calculated from the decrease of CH_3CHO concentration by UV irradiation (>300 nm; 2000 $\mu W/cm^2$; 2 h).

that the modified TiO_2 particle surface consisted of not only an amino group-donated surface but also an intact TiO_2 surface, at least in the case of an amino group density of <4 molecules/nm^2.

The photoreactivity of the modified TiO_2 was evaluated by the degradation rate of CH_3CHO. In the previous article,[13] although the anatase phase of the TiO_2 particles did not change after the reaction between the silane coupling agent and the OH groups on the outermost surface of the particle, the photoreactivity became approximately 30 times lower than that of the original TiO_2, which should be due to high coverage of the TiO_2 surface by silane coupling agents. The high coverage in the previous study should be due to crosslinking reactions among the silane coupling agents at a higher reaction temperature (120°C) than that of this study (30°C). Figure 3 shows the relationship between the density of amino groups on the TiO_2 particle surface and the rate constant calculated from the first-order rate equation[14,15] for CH_3CHO degradation by UV irradiation (wavelength, >300 nm; 2000 $\mu W/cm^2$) within 2 h. The photoreactivity did not change in the case of an amino group density of <2 molecules/nm^2 and drastically decreased with an increase in the amino group density. This result suggests that the decrease of the photoreactivity was due to the suppression of contact between CH_3CHO molecules and the intact TiO_2 surface by the silane coupling agents.

Figure 4 shows the FT-IR spectra of the original TiO_2 and the amino group-modified TiO_2 particles (amino group density, 3.0 molecules/nm^2) before and after UV irradiation (>300 nm; 2000 $\mu W/cm^2$; 2 h). Each sample was heated at 120°C for 24 h before the FT-IR measurement to remove adsorbed water. In the spectrum of the original TiO_2 [Fig. 4(a)], the band at 3692 cm^{-1} is attributed to the OH stretching vibration of the bridge-OH terminal groups on the outermost surface of TiO_2. The peaks at 3300 and 1650 cm^{-1} depend on adsorbed H_2O on the TiO_2. In the spectrum of the TiO_2 after modification with γ-APS [amino group density, 3.0 molecules/nm^2; Fig. 4(b)], the intensity of the band at 3692 cm^{-1}, attributed to the bridge-OH terminal groups of TiO_2, decreased, which corresponded to that reported in the previous article,[13] indicating the reaction of the OH groups with the silane coupling agent. An additional peak is present with respect to the original TiO_2 spectrum at 2928 cm^{-1}, indicating C—H stretching of the organic compound. As compared to the spectrum of the amino group-modified TiO_2 before UV irradiation, that after UV irradiation [Fig. 4(c)] in air did not change, which indicates that the covalent bonding did not cleave under the UV irradiation conditions within 2 h (wavelength, >300 nm; 2000 $\mu W/cm^2$). This result might be due to the slightly larger bonding energy of Si—O (369 kJ/mol) compared to that of C—C (350 kJ/mol) or C—N (291 kJ/mol) and also due to multicoupling between the silane coupling agent and the OH groups on the TiO_2 particles.

The cytotoxicity assays were conducted with the poly(AAc)-grafted silicone sheet, on which the original TiO_2 particles were physically adsorbed, and the amino-group-modified TiO_2/silicone composite (amino group density, 3.0 molecules/nm^2). Figure 5 shows the results. The number of L929 cells after incubation at 37°C for 24 h (total incubation period, 48 h) in the medium, which was exposed to each sample at 37°C for 24 h in darkness, was not statistically significant compared with that after incubation in the nontreated medium (control). This indicates that the original TiO_2/silicone and the amino-group-modified TiO_2/silicone composite sheet had no cytotoxicity to L929 cells.

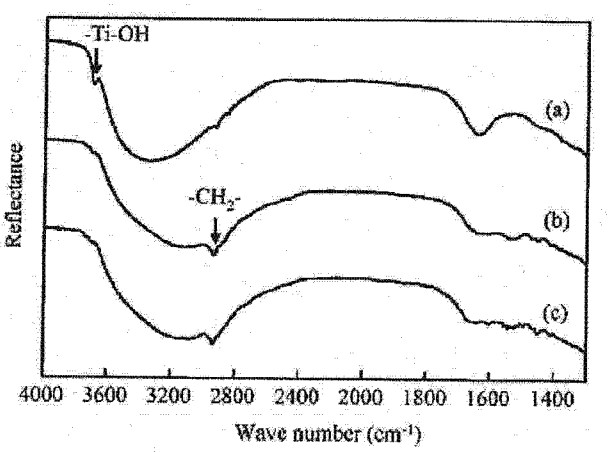

Figure 4. IR spectra of (a) original and (b,c) amino group-modified TiO_2 (amino group density, 3.0 molecules/nm^2) particles (b) before and (c) after UV irradiation (>300 nm; 2000 $\mu W/cm^2$; 2 h).

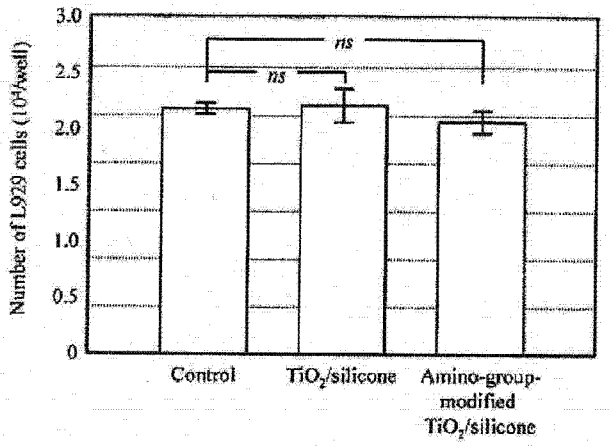

Figure 5. The number of L929 cells after incubation at 37°C for 24 h (total incubation period, 48 h; see Materials and Methods) in the medium exposed to the poly(AAc)-grafted silicone sheet, on which the original TiO_2 particles were physically adsorbed, and the amino-group modified TiO_2/silicone composite sheets (the amino group density, 3.0 molecules/nm^2). Initial number of cells, 1×10^4 cells/well. Error bars represent standard deviations of quadruplicates.

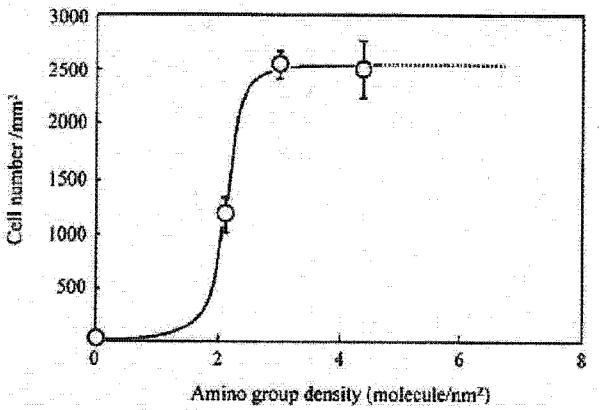

Figure 7. SEM photographs of L929 cells adhering on amino-group modified TiO_2/silicone composite sheets after incubation in 24-well multiplates (1×10^5 cells/well) at 37°C for 24 h. The amino group density on TiO_2 particle surfaces (molecules/nm^2): (a,a') 0; (b,b'); 2.1; (c,c') 3.0. (a,b,c) low magnification; (a',b',c') high magnification.

In order to evaluate the cell adhesion activity of the TiO_2/silicone composite, L929 cells were scattered and incubated on the composite sheet for 24 h at 37°C. Figures 6 and 7 show, respectively, SEM photographs and the number of the L929 cells adhering on the control sample [the poly(AAc)-grafted silicone sheet, on which the original TiO_2 particles were physically adsorbed] and the composite sheet with the TiO_2 having different amino group densities. In the case of the control sample shown in Figure 6(a), few cells adhered. Judging from the cytotoxicity assay shown in Figure 5, the lack of cell adhesion on the control sample was not due to the cytotoxicity of the TiO_2/silicone, but high hydrophilicity of the original TiO_2 surface. On the other hand, the cells dramatically adhered on the composite surface compared with the control sample, and the number of cells adhering on the composite sheet increased with the increase in the amino group density (Fig. 7). This is because cationic groups such as amino groups promote initial cell adhesion and growth.[17] In photographs with higher magnification [Fig. 6(b',c')], the cells elongated their needlelike

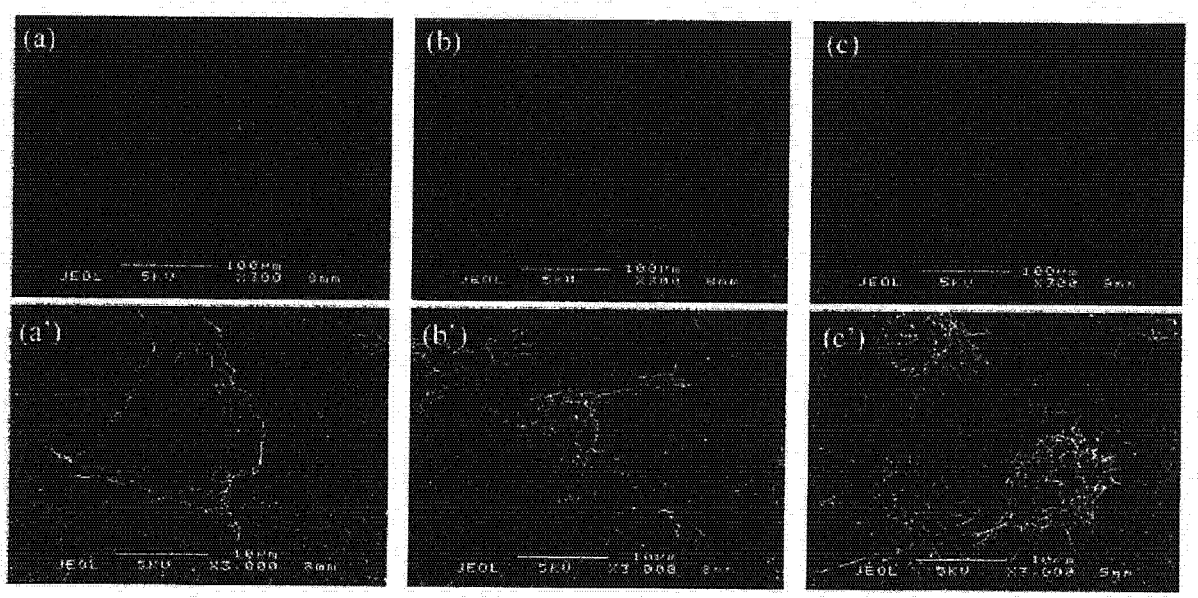

Figure 6. Relationship between the amino group density on the TiO_2 particle surfaces and the number of L929 cells adhering on the TiO_2/silicone composite sheets after incubation in 24-well multiplates (1×10^5 cells/well) at 37°C for 24 h.

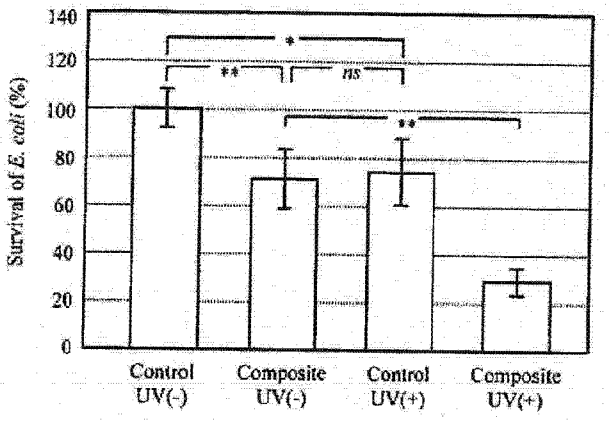

Figure 8. Effect of UV irradiation (360 nm; 470 $\mu W/cm^2$; 120 min) on the number of *E. coli* cells on the amino group-modified TiO_2/silicone composite sheet. The amino group density on the TiO_2 particle surfaces was 3.0 molecules/$nm.^2$ Error bars = SD of quadruplicates ($^*p < 0.05$; $^{**}p < 0.01$).

microspikes restrictedly onto the amino group-modified TiO_2 surface. The microspikes from the cells had no affinity for the bottom of the poly(AAc)-grafted silicone surface having high hydrophilicity[13] and the original TiO_2 particles [Fig. 6(a')].

From the above results shown in Figures 3 and 7, the optimum density of amino groups for both photoreactivity and cell adhesiveness was estimated to be 2.0–4.0 molecules/nm^2. Therefore, the TiO_2/silicone composite consisting of the TiO_2 particles (amino group density, 3.0 molecules/nm^2) was used for the antibacterial activity test. It is worth pointing out that the TiO_2/silicone composite showed the same flexibility as the original silicone sheet, that is, the chemical surface modification with TiO_2 particles showed no mechanical disadvantage, which was similar to the HAp/silicone composite.[12]

The antibacterial activity of the optimum amino group-modified TiO_2/silicone composite (amino group density, 3.0 molecules/nm^2) was estimated from survival ratio of *E. coli* bacteria on the composite sheet after UV irradiation (wavelength, 360 nm; 470 $\mu W/cm^2$; 2 h), which is shown in Figure 8. In the case of the control test after UV irradiation, the direct antibacterial effect of UV rays was slightly observed. On the other hand, in the case of the composite sheet, 29% decrease in the number of *E. coli* bacteria was observed before UV irradiation, and the number of bacteria decreased significantly after UV irradiation (72%). These results indicate a bacteria adsorption onto the optimum amino group-modified TiO_2/silicone composite and effective antibacterial activity by photoexcited TiO_2 under UV irradiation. It is expected that a completely destroying of bacteria will be obtained by optimizing the surface area of the composite sheets and UV irradiation conditions such as wavenumber, intensity, and irradiation time of UV light. It is worth pointing out that the covalent bonding was not cleaved under the UV irradiation (wavelength, >300 nm; 2000 $\mu W/cm^2$; 2 h) as shown in Figure 4. Therefore, the composite developed here is expected to show antibacterial activity under UV irradiation while maintaining tissue adhesiveness.

In conclusion, the amino group density on the TiO_2 particle surface was optimized in order to develop a composite consisting of amino group-modified TiO_2 particles and a flexible silicone sheet through covalent linkage, having both photoreactivity and cell adhesiveness. The photoreactivity of the TiO_2 particles decreased with an increase in the amino group density on the TiO_2 particle surfaces. On the other hand, the number of L929 cells adhering on the composite sheet increased with an increase in the amino group density. Based on the above results, the optimum density of amino groups for both photoreactivity and cell adhesiveness was estimated to be 2.0–4.0 molecules/nm^2, and a composite consisting of TiO_2 particles having that optimum density was developed. Irradiation of UV light onto *E. coli* on the optimum amino group-modified TiO_2/silicone sheet showed an effective antibacterial activity of the composite. The composite developed here could be utilized for elastic percutaneous or subcutaneous devices having good tissue adhesiveness and an antibacterial effect.

References

1. Fujishima A, Honda K. Electrochemical photolysis of water at a semiconductor electrode. Nature 1972;238:37–38.
2. Ollis DF, Pelizetti E, Serpone N. Destruction of water contaminants. Environ Sci Technol 1991;25:1523–1529.
3. Uchida H, Itoh S, Yoneyama H. Photocatalytic decomposition of propyzamide using TiO_2 supported on activated carbon. Chem Lett 1993:1995–1998.
4. Heller A. Chemistry and applications of photocatalytic oxidation of thin organic films. Acc Chem Res 1995;28:503–508.
5. Sitkiewitz S, Heller A. Photocatalytic oxidation of benzene and stearic acid on sol-gel derived TiO_2 thin films attached to glass. New J Chem 1996;20:233–241.
6. Cai R, Kubota Y, Shiumi T, Sakai H, Kashimoto K, Fujishima A. Induction of cytotoxicity by photoexcited TiO_2 particles. Cancer Res 1992;52:2346–2348.
7. Sunada K, Kikuchi Y, Hashimoto K, Fujishima A. Bactericidal and detoxification effects of TiO_2 thin film photocatalysts. Environ Sci Technol 1998;32:726–728.
8. Morioka T, Saito T, Nara Y, Onoda K. Antibacterial action of powdered semiconductor on serotype g Streptococcus mutans. Caries Res 1988;22:230–231.
9. Bischoff F, Bryson G. Tissue reaction to and fate of parenterally administered titanium dioxide. I. The intraperitoneal site in male Marsh-Buffalo mice. Res Commun Chem Pathol Pharmacol 1982;38:279–290.
10. Bernard BK, Osheroff MR, Hofman A, Mennear JH. Toxicology and carcinogenesis studies of dietary titanium dioxide-coated

mica in male and female Fischer 344 rats. J Toxicol Environ Health 1989;28:415–426.
11. Furuzono T, Sonoda K, Tanaka J. A hydroxyapatite coating covalently linked onto a silicone implant materials. J Biomed Mater Res 2001;56:9–12.
12. Furuzono T, Wang P, Korematsu A, Miyazaki K, Oido-Mori M, Kowashi Y, Ohura K, Tanaka J, Kishida A. Physical and biological evaluations of sintered hydroxyapatite/silicone composite with covalent bonding for a percutaneous implant material. J Biomed Mater Res B Appl Biomater 2003;65B;217–226.
13. Furuzono T, Iwasaki M, Yasuda S, Korematsu A, Yoshioka T, Ito S, Kishida A. Photoreactivity and cell adhesiveness of amino-group-modified titanium dioxide nano-particles on silicone substrate coated by covalent linkage. J Mater Sci Lett 2003;22: 1737–1740.
14. Anderson C, Bard AJ. Improved photocatalytic activity and characterization of mixed TiO_2/SiO_2 and TiO_2/Al_2O_3 Materials. J Phys Chem 1997;99:2611–2616.
15. Tada H. Photoinduced oxidation of methylsiloxane monolayers chemisorbed on TiO_2. Langmuir 1996;12:966–971.
16. Morimoto T, Nagao M, Tukuda F. The relation between the amounts of chemisorbed and physisorbed water on metal oxides. J Phys Chem 1969;73:243–248.
17. Rosen JJ, Gibbons DF, Culp LA. In: Andrade JD, editor, ACS Symposium Series 31. Washington, DC: American Chemical Society; 1976. p 329–343.